

INPOP: EVOLUTION, APPLICATIONS, AND PERSPECTIVE

A. Fienga¹, J. Laskar², A. Verma¹, H. Manche² and M. Gastineau²

Abstract. The INPOP ephemerides have known several improvements and evolutions since the first INPOP06 release in 2008 (Fienga et al. 2008). In 2010, anticipating the IAU 2012 resolutions, adjustment of the gravitational solar mass with a fixed astronomical unit (AU) has been for the first time implemented in INPOP10a (Fienga et al. 2011) together with improvements in the asteroid mass determinations. With the latest INPOP10e version (Fienga et al. 2012), such advancements have been enhanced and studies about solar corona have also been investigated (Verma et al. 2012). The use of planetary ephemerides for several physical applications are presented here from electronic densities of solar slow and fast winds to asteroid mass determinations and tests of general relativity operated with INPOP10a. Perspectives will also be drawn especially related to the analysis of the Messenger spacecraft data for the planetary orbits and future computation of the time variations of the gravitational mass of the sun.

Keywords: Planetary ephemerides, numerical integration, space missions, tests of general relativity, asteroid masses

1 Introduction

Since 2006, INPOP (Integration Numerique Planetaire de l'Observatoire de Paris) has become an international reference for space navigation (to be used for the GAIA mission navigation and the analysis of the GAIA observations) and for scientific research in dynamics of the solar system objects and in fundamental physics. A first version of INPOP, INPOP06, was published in 2008 ((Fienga et al. 2008)). This version is very close to the reference ephemerides of JPL in its dynamic model and in its fit procedure. With MEX and VEX tracking data provided by ESA, lunar laser ranging observations and the development of new planetary and moon ephemeris models and new adjustment methods, INPOP08 (Fienga et al. 2009) and INPOP10a (Fienga et al. 2011b) were constructed. These versions of INPOP have established INPOP at the forefront of global planetary ephemerides because its precision in terms of extrapolation to the position of planets is equivalent to the JPL ephemerides. Its dynamic model follows the recommendations of the International Astronomical Union (IAU) in terms of i) compatibility between time scales (TT, TDB), ii) metric in the relativistic equations of motion (consistency in the computation of the position of the barycenter of the solar system) and iii) in the fit of the sun gravitational mass with a fixed AU.

INPOP provides to the user, positions and velocities of the planets, the moon, the rotation angles of the earth and the moon as well as TT-TDB chebychev polynomials at <http://www.imcce.fr/inpop>. INPOP10a was the first planetary ephemerides in the world built up with a direct estimation of the gravitational mass of the sun with a fixed astronomical unit instead of the traditional adjustment of the AU scale factor. With INPOP10a, we have demonstrated the feasibility of such determination helping the IAU of taking the decision of fixing the astronomical unit (see resolution B2 of the 35th IAU general assembly, 2012).

The INPOP01e (Fienga et al. 2012) is the latest INPOP version developed for the Gaia mission final release and available for users. Compared to INPOP10a, new sophisticated procedures related to the asteroid mass determinations have been implemented: bounded value least squares have been associated with a-priori sigma estimators (Kuchynka 2010; Fienga et al. 2011a) and solar plasma corrections (Verma et al. 2012). Very recent Uranus observations provided by Viera Martins & Camargo (2012) have been added as well as positions of Pluto deduced from HST (Tholen et al. 2008).

¹ Institut UTINAM-CNRS 6213, Université de Franche-Comté, Besançon, France

² Astronomie et Systèmes Dynamiques, IMCCE-CNRS UMR8028, Paris, France

Table 1. Values of parameters obtained in the fit of INPOP10e and INPOP10a to observations.

	INPOP10e $\pm 1\sigma$	INPOP06 $\pm 1\sigma$	DE423 $\pm 1\sigma$
$(\text{EMRAT}-81.3000) \times 10^{-4}$	(5.700 ± 0.020)	5.6	(5.694 ± 0.015)
$J_2^\odot \times 10^{-7}$	(1.80 ± 0.25)	(1.95 ± 0.5)	1.80
$\text{GM}_\odot - 132712440000 \text{ [km}^3 \cdot \text{s}^{-2}\text{]}$	(50.16 ± 1.3)	17.987	40.944
$\text{AU} - 1.49597870700 \times 10^{11} \text{ [m]}$	9.0	9.0	(-0.3738 ± 3)
$[\text{M}_\odot / \text{M}_{\text{EMB}}] - 328900 \times 10^{11}$	5.5253 ± 0.0027	5.6140	$5.5915 \pm \text{NC}$

Adjustment of the gravitational mass of the sun is performed as recommended by the IAU resolution B2 as well as the sun oblateness (J_2), the ratio between the mass of the earth and the mass of the moon (EMRAT) and the mass of the Earth-Moon barycenter. Estimated values are presented on Table 1.

Masses of the planets have been as well updated to the IAU best estimated values (Luzum et al. 2012).

Thanks to the added solar corrections and to the improvement in the fit procedure, 152 asteroid masses have been estimated (see section 3). Comparisons to other planetary ephemerides, postfit and extrapolated residuals are discussed in section 2.

2 Estimation of uncertainties

2.1 Comparisons to other planetary ephemerides

In order to better estimate the INPOP10e uncertainties, comparisons are made between INPOP10e, INPOP10a and the JPL DE423 (Folkner 2010) in spherical coordinates (table 2) for the planets relative to the earth and in cartesian coordinates (table 3) for the earth relative to the solar system barycenter in the ICRF (also called BCRS) over a period of 20 years before and after J2000. With these figures, differences in the dynamic model, fitting procedures and data sample can be impacted on planetary positions and velocities for an interval of time corresponding to the most accurate data sets.

The DE423 ephemerides have been fitted on a data set similar to the INPOP10e one. Fitting procedures differ with less asteroid masses adjusted in DE423 (63) and smoother behavior in the Mars residuals during the fitted period (see table 1). INPOP10e differs from INPOP10a by new corrections in the Messenger data, new implementation in the fit of the asteroid masses and in the correction of the solar plasma, and the use of very recent observations of Uranus (Viera Martins & Camargo 2012) inducing modifications in the weighting schema of the adjustment. Differences between INPOP10e, DE423 and INPOP10a can be seen as good estimations of the state-of-art uncertainties of planetary ephemerides.

As expected, the uncertainties of the positions of inner planets are quite smaller than those obtained for the outer planets. This can easily be explained by the use in the ephemeris construction of high accurate data deduced from the tracking of inner planet orbiters during the past 40 years.

For Jupiter, the uncertainty in geocentric distance is about 1 km but the angular differences are not quite similar from one ephemeris to another: from 10 mas with INPOP10a to less than 1 mas with DE423.

Due to these important variations and to the expected lack of accurate Jupiter observations in the near future, the accuracy of the Jupiter orbit is very likely to degrade in the coming years. For Saturn, the ephemerides give more consistent results reflecting the important role of the Cassini observations in the Saturn orbit determination. For Uranus, Neptune and Pluto, the important differences illustrate the lack of accurate estimations of distances and angular positions for these objects.

Differences in the earth BCRS positions and velocities obtained for several planetary ephemerides (see table 3) are about 1 kilometer in positions and smaller than $0.1 \text{ mm}\cdot\text{s}^{-1}$ in velocities. Comparisons between DE423 and DE421 (Folkner et al. 2008) which differ mainly by the data sample are equivalent to those obtained with the two consecutive INPOP versions (INPOP10e and INPOP10d (Verma et al. 2012)). In the case of INPOP10e and INPOP10a, these figures can be explained up to 85 % by differences in the estimation of the gravitational mass of the sun.

2.2 Comparisons to observations, extrapolation and link to the ICRF

The INPOP10e observational sample has 3 times more data than the INPOP06 one (the first INPOP release) which ended in 2005.45. The statistical distribution of the supplementary data sets is not uniform and is mostly constituted with MEX and VEX observations (60 %). However, the two flyby points of Uranus and Neptune and the five flybys of Jupiter are of crucial importance for the accuracy of these orbits. The three positions of Mercury deduced from the Messenger flybys play also an important role for the Mercury orbit determination even if their distribution in time was very limited (less than 2 years).

On table 1 are given some examples of postfit and extrapolated residuals obtained with INPOP10e and other ephemerides. For Mars, INPOP10e faces an improvement of the extrapolated residuals compared to INPOP10a and obtains the same level of accuracy as the JPL DE423. The Saturn residuals presented in table 1 are good examples of the improvement of the outer planet orbits obtained with INPOP10e compared to the previous INPOP versions. In particular, a reduction of a factor more than 10 is obtained in Cassini range residuals. This improvement is also confirmed with the Uranus and Neptune flyby residuals. By providing measured distances between the earth and the outer planets, the flyby data brought new informations to the fit when only optical observations were used in the INPOP06 and INPOP08 adjustments. As a result, one can notice the satisfactory INPOP06 residuals obtained for the outer planet accurate spacecraft tracking data (Cassini in table 1) in right ascension and declination (at the level of the accuracy of the optical data used in the INPOP06 fit) but the very poor estimations in distances.

For Jupiter, the expected accuracy of the ephemerides will not be better than the postfit residuals obtained by comparison to flyby positions which reach up about 2 kilometers (see Fig. 1). Unfortunately, no direct accurate observation of Jupiter (such as radio or VLBI tracking of a spacecraft in its vicinity) are planned in the near future in order to maintain the constraints over the Jupiter orbit. Calibration of possible Jupiter orbit degradation would only be partially possible through indirect constraints from Cassini Solstice mission, Dawn, Messenger, present and future Mars orbiters. However, contrary to Jupiter, new Saturn positions would be obtained during the Cassini Solstice mission through 2017 and would then be helpful for constraining the Saturn orbit in the coming years.

For the inner planets, the orbits are very well constrained thanks to spacecraft tracking data of Mars orbiters, VEX and Messenger missions. However, we note a rapid degradation of the Mars orbit accuracy as estimated by comparison between planetary ephemerides and observed MEX distances not included in the fit of the ephemerides. Such comparisons are called extrapolation in the top charts of the Fig. 1. The differences between estimated distances and the observed one reach up to 30 meters after 32 months and are mainly due to un-modeled perturbations of main-belt asteroids.

Even if not seen as a major planet anymore, Pluto orbit is also included in the INPOP planetary ephemerides. For our latest version, we work on the improvement of the Pluto orbit in including stellar occultations (as in INPOP10a) but also positions of the Pluto-Charon barycentric system obtained in 2008 with HST by Tholen et al. (2008). In the opposite of DE423, INPOP10e shows un-biased residuals in right ascension and declination as one can see on Fig. 1.

The tie between INPOP ephemerides and the ICRF (McCarthy & Petit 2003) is maintained by the use of VLBI differential observations of spacecraft relative to ICRF sources. Such methods give milliarcsecond (mas) positions of a spacecraft orbiting a planet directly in the ICRF. Combining such VLBI observations with spacecraft navigation, positions of planets can be deduced relatively to the ICRF sources. The link between modern planetary ephemerides and the ICRF is then obtained at the accuracy of the VLBI localization of the space missions. Based on the most recent Mars, VEX and Cassini VLBI observations, the link between the INPOP10e reference frame and the ICRF is maintained with an accuracy of about 1 mas for the last 10 years.

3 Applications

3.1 Solar physics

As one can see on the left-hand side chart of the Fig. 2, range observations of MGS, MEX and VEX spacecraft were highly affected by solar plasma perturbations during solar conjunctions, but also before and after these critical periods. In the opposite side of the spectrum, solar physicists are interested in characterizing electronic densities of two specific area on the sun surface: the regions in which dominates a slow wind (mainly following the magnetic neutral line) and the regions (higher in solar latitudes) corresponding to fast winds (Schwenn & Marsch 1990, 1991). By analyzing the path of the radiometric signal from the spacecraft to the earth, it is

Table 2. Maximum differences between INPOP10e, INPOP10a and DE423 from 1980 to 2020 in spherical geocentric coordinates and distances.

Geocentric Differences	INPOP10e - INPOP10a			INPOP10e - DE423		
	1980-2020			1980-2020		
	α	δ	ρ	α	δ	ρ
	mas	mas	km	mas	mas	km
Mercury	1.4	3.1	0.6	1.58	1.7	0.65
Venus	0.27	0.43	0.021	0.85	0.42	0.045
Mars	1.26	0.37	0.185	2.1	0.62	0.47
Jupiter	4.13	9.94	0.88	0.81	0.74	1.11
Saturn	0.54	0.52	0.51	0.82	0.53	1.82
Uranus	226.9	120.2	1370	98.1	38.9	359.73
Neptune	12.6	6.5	1081	51.0	91.3	2054.8
Pluton	25.53	154.8	3447.1	703.2	152.7	37578.6

Table 3. Maximum differences between INPOP10e and other planetary ephemerides from 1980 to 2020 in cartesian coordinates of the earth in the BCRS.

Earth Barycentric Differences	XYZ	VxVyVz
	km	mm.s ⁻¹
INPOP10e - INPOP10a	-1.0	0.050
INPOP10e - DE423	0.84	0.113
DE423-DE421	0.37	0.070
INPOP10e-INPOP10d	0.34	0.050

possible to estimate such electronic densities for the two regions during the ingress and the egress parts of the signal and for different phases of the solar activity (Verma et al. 2012). On the right-hand chart of the Fig. 2, the distributions of MGS, MEX and VEX analyzed data in slow and fast wind regions are plotted and the obtained electronic densities for the two regions are also given. After the estimation of the electronic densities, solar plasma corrections were applied to the radiometric signal from the Mars and Venus orbiters, as one can see on the left-hand side chart of the Fig. 2. Such corrections allow to re-introduce in the INPOP fit 8% of supplementary data, previously rejected, and then to improve the extrapolation capabilities of INPOP10e and the asteroid mass determinations (Verma et al. 2012).

3.2 Asteroid masses

Due to the perturbations of the main belt asteroids over the Mars and the earth orbits, asteroid mass determinations deduced from the construction of planetary ephemerides and the analysis of the high accurate Mars orbiter tracking distances are done regularly (Konopliv et al. 2011; Fienga et al. 2011a; Somenzi et al. 2010; Konopliv et al. 2006). However, the inversion problem is here very complex as only less than 50 asteroid masses (to be compared with the 300 asteroids included in the dynamic model of the ephemeris) are known and as all the perturbations cumulate over the Mars geocentric distances. Sophisticated procedures have been tested for years (Standish & Fienga 2002; Kuchynka 2010; Kuchynka et al. 2010). Thanks to the implementation of bounded value least squares associated with a-priori sigma estimators and to the corrections of solar plasma perturbations, we have been able to estimate 152 asteroid masses presented in Fienga et al. (2012). This release is quite satisfactory: comparisons between INPOP10e values and values obtained by other authors either by planetary ephemeris construction (Konopliv et al. 2011; Kuchynka 2012) or by close-encounter methods (Zielenbach 2011; Baer et al. 2011) are indeed in good agreement. As one can see on Fig. 3, asteroids inducing more than 7 meter perturbations over the Mars-earth distances have very consistent densities. This limit is consistent with the dispersion of the postfit residuals presented on Fig. 1 which is about 9 meters for all the data sample and 4 meters out of the conjunction periods. Furthermore, for small perturbers, and contrarily to the previous

INPOP versions, INPOP10e does not provide unrealistic densities, smaller than 0.5 g.cm^{-3} or greater than 6 g.cm^{-3} .

3.3 Tests of fundamental physics

Thanks to the high precision obtained by INPOP08 and INPOP10a, computations have also included determinations of the PPN parameter β with considerable precision and estimates of the perihelion advances of the 8 planets of the solar system. No new advance and no β -deviation of the unit could be clearly demonstrated, confirming the validity of general relativity to the level of 10^{-5} (Fienga et al. 2010, 2011b). Combined estimations of PPN parameters β and γ were also obtained with great accuracy using INPOP10a as well as sharp constraints on supplementary advances of nodes and perihelia of the planets. These latest estimations give stringent constraints on cosmological models of gravity such as MOND (Blanchet & Novak 2011). Tests of acceptable supplementary Pioneer-like accelerations were also done and confronted to the most accurate observations of outer planets. As one can see on the Fig. 3, only an acceleration with an amplitude smaller $5.10^{-13} \text{ m.s}^{-2}$ is compatible with the observed geocentric Saturn distances deduced from the Cassini tracking data.

4 Conclusions

Planetary ephemerides are not a only crucial tool for celestial mechanics or the preparation of space missions. They can also play an important role in testing gravity, studying the asteroid physics by estimating their masses or in solar physics with the analysis of the solar corona signatures over radiometric tracking observations of planet orbiters. We present here the latest INPOP version. It appears to be as accurate as the JPL DE ephemerides and allows several applications in solar physics, planetology and gravity testing. At the end of 2012, the analysis of the Messenger tracking data should be completed and implemented in INPOP. These new observations would be crucial especially for gravity tests. We will also implement the estimation of possible variation of the gravitational mass of the sun. This parameter would give stringent limits to theoretical developments predicting variations with time of the gravitational constant. More observations of Saturn deduced from the Solstice extended Cassini mission should also be available. These data would be very helpful to maintain the accuracy of the outer planet orbits.

References

- Baer, J., Chesley, S. R., & Matson, R. 2011, *AJ*, 212
- Blanchet, L. & Novak, J. 2011, *MNRAS*, 412, 2530
- Fienga, A., Kuchynka, P., Laskar, J., Manche, H., & Gastineau, M. 2011a, in EPSC-DPS Joint Meeting 2011, 1879
- Fienga, A., Laskar, J., Kuchynka, P., et al. 2010, American Astronomical Society, IAU Symposium #261. Relativity in Fundamental Astronomy: Dynamics, Reference Frames, and Data Analysis 27 April - 1 May 2009 Virginia Beach, VA, USA, #6.02; *Bulletin of the American Astronomical Society*, Vol. 41, p.881, 261, 602
- Fienga, A., Laskar, J., Manche, H., Gastineau, M., & Verma, A. 2012, DPAC INPOP final release: INPOP10e, ArXiv e-prints
- Fienga, A., Laskar, J., Manche, H., et al. 2011b, *Celestial Mechanics and Dynamical Astronomy*, 111, 363
- Fienga, A., Laskar, J., Morley, T., et al. 2009, *A&A*, 507, 1675
- Fienga, A., Manche, H., a. L. J., & Gastineau, M. 2008, *A&A*, 477, 315
- Folkner, W. 2010, JPL Interoffice Memorandum IOM 343.R-10-001: Planetary Ephemeris DE423 fit to Messenger encounters with Mercury, Tech. rep., JPL Interoffice Memorandum IOM 343.R-10-001
- Folkner, W. M., Williams, J. G., & Boggs, D. H. 2008, jPL Interoffice Memorandum IOM 343R-08-003
- Konopliv, A. S., Asmar, S. W., Folkner, W. M., et al. 2011, *Icarus*, 211, 401
- Konopliv, A. S., Yoder, C. F., Standish, E. M., Yuan, D.-N., & Sjogren, W. L. 2006, *Icarus*, 182, 23
- Kuchynka, P. 2010, PhD in astronomy, Observatoire de Paris
- Kuchynka, P. 2012, private communication
- Kuchynka, P., Laskar, J., Fienga, A., & Manche, H. 2010, *A&A*, 514, A96+
- Luzum, B., Capitaine, N., Fienga, A., et al. 2012, *Transactions of the International Astronomical Union, Series A*, 28, 50
- McCarthy, D. D. & Petit, G. 2003, IERS Technical Note No 32, Tech. rep., IERS Convention Centre, <http://www.iers.org/iers/publications/tn/tn32/>
- Schwenn, R. & Marsch, E. 1990, *Physics of the Inner Heliosphere I.: Large-Scale Phenomena*. (Springer)

- Schwenn, R. & Marsch, E. 1991, *Physics of the Inner Heliosphere II.: Particles, Waves and Turbulence.* (Springer)
- Somenzi, L., Fienga, A., Laskar, J., & Kuchynka, P. 2010, *Planetary and Space Science*, 58, 858
- Standish, E. M. & Fienga, A. 2002, *A&A*, 384, 322
- Tholen, D. J., Buie, M. W., Grundy, W. M., & Elliott, G. T. 2008, *AJ*, 135, 777
- Verma, A. K., Fienga, A., Laskar, J., et al. 2012, ArXiv e-prints
- Viera Martins, R. & Camargo, J. I. B. 2012, private communication
- Zielenbach, W. 2011, *AJ*, 142, 120

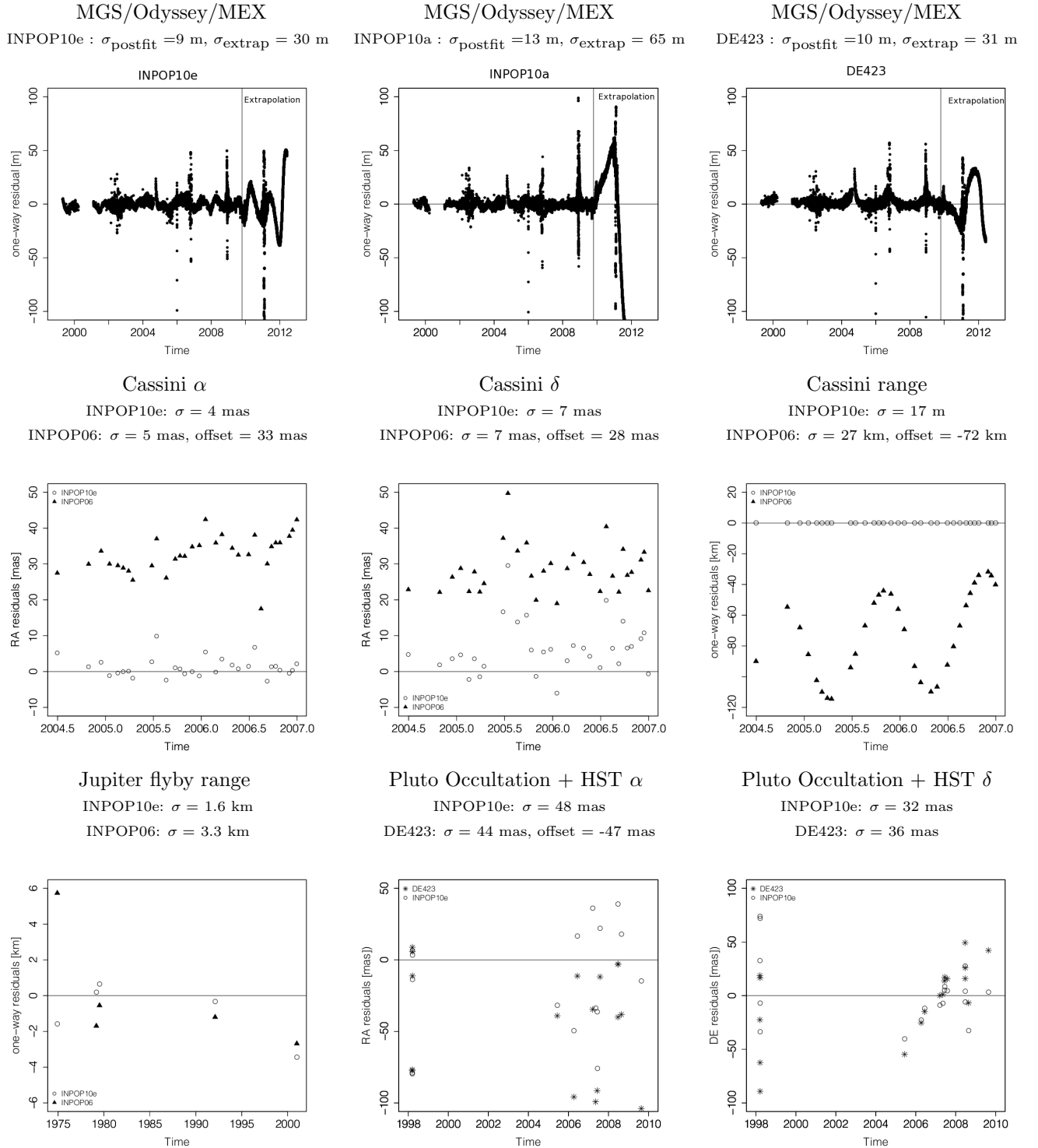


Fig. 1. Some examples of postfit and extrapolated residuals obtained with INPOP10e, INPOP10a, INPOP06 and DE423. The given σ (resp. offset) are the 1- σ dispersion (resp. mean) of the residual distributions. Only statistically meaningful offsets are given.

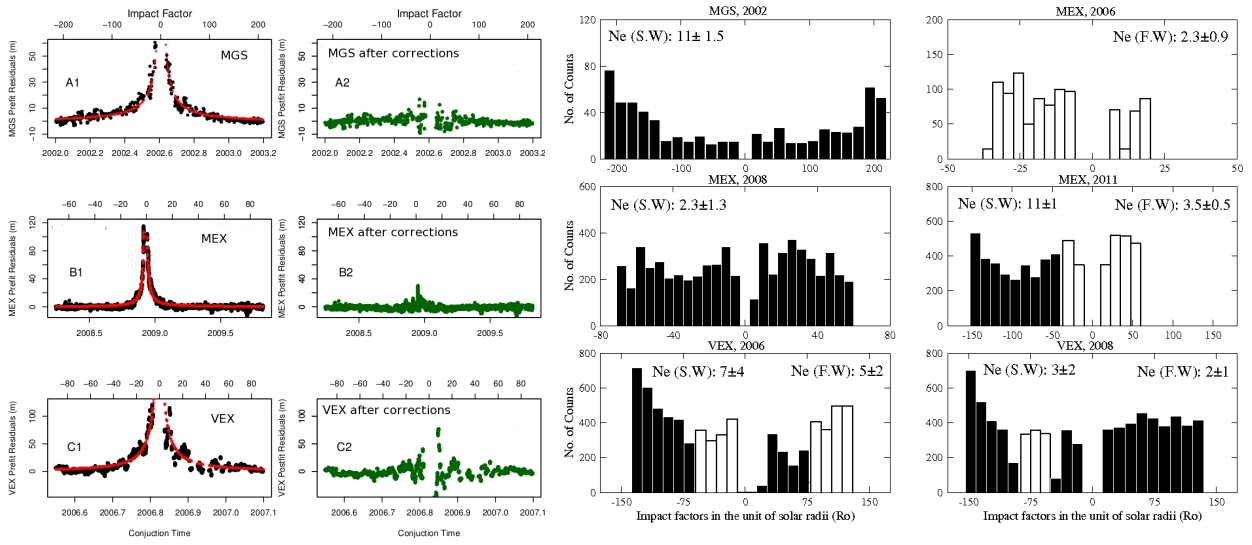


Fig. 2. Solar physics applications: a) Corrections of solar plasma applied to MGS, MEX and VEX range measurements. b) Histograms of the distributions of MGS, MEX and VEX data during solar conjunctions in slow (black) and fast (white) wind regions. Are also given the values of the obtained electronic density (N_e) at 1 AU in electrons.cm^{-3} .

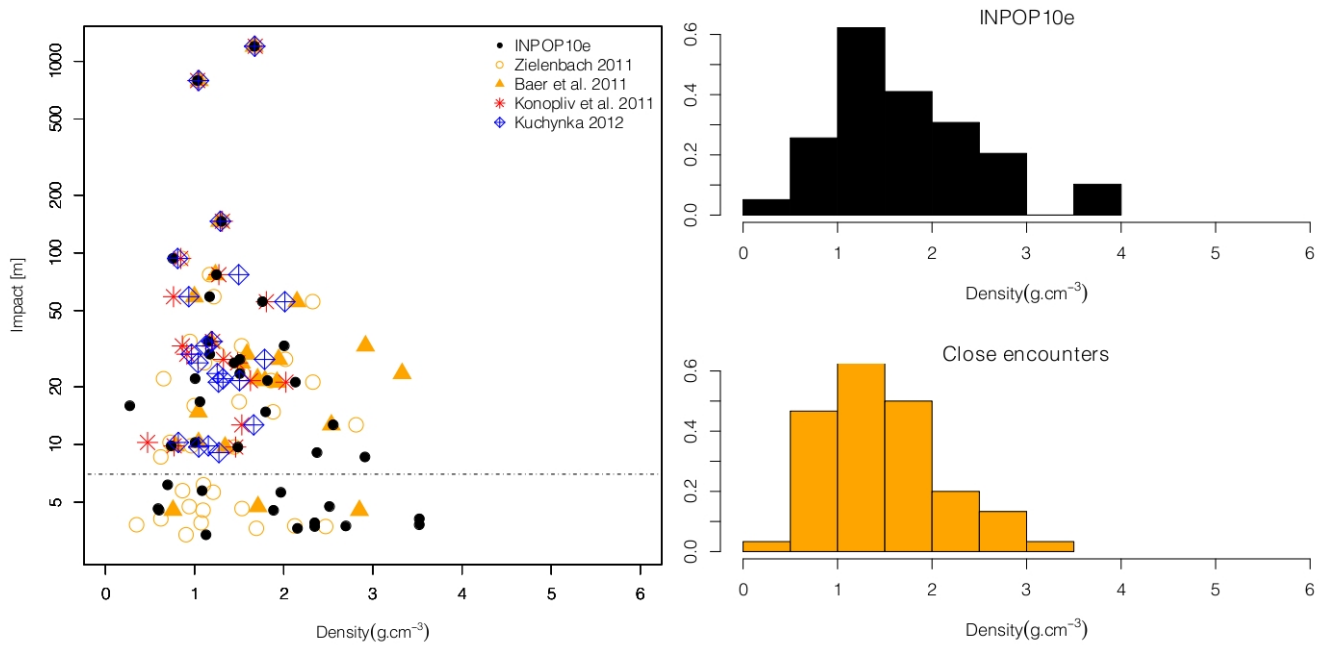


Fig. 3. INPOP10e Asteroid mass determination: a) INPOP10e asteroid densities compared to other published values versus the impact of the asteroids over the Mars-earth distances during a 1970 to 2012 period. b) Histograms of distribution of the asteroid densities obtained with INPOP10e and with close-encounter methods (right-hand side chart).

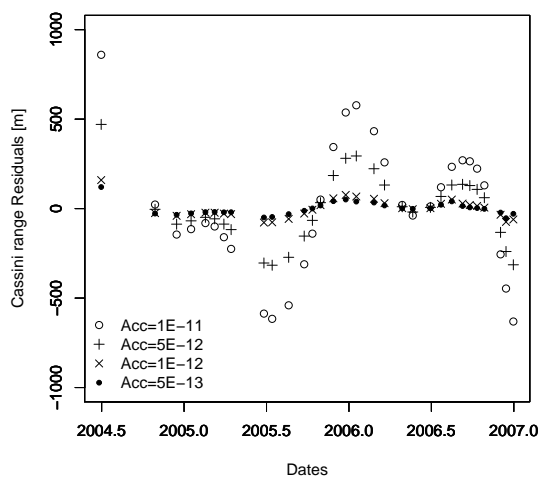


Fig. 4. Differences between Cassini range data and earth-Saturn distances obtained with supplementary Pioneer-like acceleration on the Saturn orbit.